Schizophrenia Research 206 (2019) 370–377

Contents lists available at ScienceDirect

Schizophrenia Research

journal homepage: www.elsevier.com/locate/schres

Altered functional connectivity between sub-regions in the thalamus and cortex in schizophrenia patients measured by resting state BOLD fMRI at 7T

Jun Hua [a,b,*], Nicholas I.S. Blair [c], Adrian Paez [b], Ann Choe [a,b], Anita D. Barber [d,e], Allison Brandt [f], Issel Anne L. Lim [a,b], Feng Xu [a,b], Vidyulata Kamath [g], James J. Pekar [a,b], Peter C.M. van Zijl [a,b], Christopher A. Ross [f,h,i], Russell L. Margolis [f,h]

[a] The Russell H. Morgan Department of Radiology and Radiological Science, Division of MR Research, The Johns Hopkins University School of Medicine, Baltimore, MD, USA
[b] F.M. Kirby Research Center for Functional Brain Imaging, Kennedy Krieger Institute, Baltimore, MD, USA
[c] Department of Biomedical Engineering, Johns Hopkins University, Baltimore, MD, USA
[d] Center for Psychiatric Neuroscience, Feinstein Institute for Medical Research, Manhasset, New York, USA
[e] Department of Psychiatry, Zucker School of Medicine at Hofstra/Northwell, Hempstead, New York, USA
[f] Department of Psychiatry and Behavioral Sciences and Program in Cellular and Molecular Medicine, Johns Hopkins University School of Medicine, Baltimore, MD, USA
[g] Department of Psychiatry and Behavioral Sciences, Johns Hopkins University School of Medicine, Baltimore, MD, USA
[h] Department of Neurology, Johns Hopkins University School of Medicine, Baltimore, MD, USA
[i] Department of Neuroscience and Pharmacology, Johns Hopkins University School of Medicine, Baltimore, MD, USA

ARTICLE INFO

Article history:
Received 17 May 2018
Received in revised form 11 October 2018
Accepted 20 October 2018
Available online 6 November 2018

Keywords:
Imaging
Biomarker
High field
Psychosis
Thalamus

ABSTRACT

The thalamus is a small brain structure that relays neuronal signals between subcortical and cortical regions. Abnormal thalamocortical connectivity in schizophrenia has been reported in previous studies using blood-oxygenation-level-dependent (BOLD) functional MRI (fMRI) performed at 3T. However, anatomically the thalamus is not a single entity, but is subdivided into multiple distinct nuclei with different connections to various cortical regions. We sought to determine the potential benefit of using the enhanced sensitivity of BOLD fMRI at ultra-high magnetic field (7T) in exploring thalamo-cortical connectivity in schizophrenia based on subregions in the thalamus. Seeds placed in thalamic subregions of 14 patients and 14 matched controls were used to calculate whole-brain functional connectivity. Our results demonstrate impaired thalamic connectivity to the prefrontal cortex and the cerebellum, but enhanced thalamic connectivity to the motor/sensory cortex in schizophrenia. This altered functional connectivity significantly correlated with disease duration in the patients. Remarkably, comparable effect sizes observed in previous 3T studies were detected in the current 7T study with a heterogeneous and much smaller cohort, providing evidence that ultra-high field fMRI may be a powerful tool for measuring functional connectivity abnormalities in schizophrenia. Further investigation with a larger cohort is merited to validate the current findings.

1. Introduction

The thalamus is an important deep gray matter structure that relays information between subcortical and cortical regions. Altered thalamocortical connectivity has been reported in schizophrenia (SCZ) (Anticevic et al., 2014; Anticevic et al., 2015; Cetin et al., 2014; Klingner et al., 2014). The thalamus can be subdivided into multiple distinct nuclei with different anatomical connections to various cortical regions (Behrens et al., 2003a; Behrens et al., 2003b). To better assess the relationship between schizophrenia and thalamocortical connectivity, it is therefore critical to investigate the functional connectivity between sub-regions in the thalamus and the cortex, rather than averaging connectivity across the entire thalamus. Indeed, findings using 3.0 Tesla (3T) MRI support a differential connectivity between specific subregions and the cortex (Anticevic et al., 2014; Anticevic et al., 2015). As the sensitivity of blood-oxygenation-level dependent (BOLD) functional MRI (fMRI) is expected to show a supra-linear enhancement with field strength (Uludag et al., 2009), ultra-high field (7.0 Tesla, or 7T, and beyond) BOLD fMRI provides a powerful tool for the investigation of the functional connectivity of these small subthalamic regions, potentially using much smaller sample sizes than are

* Corresponding author at: Department of Radiology, Johns Hopkins University School of Medicine, F.M. Kirby Research Center for Functional Brain Imaging, Kennedy Krieger Institute, 707 N Broadway, Baltimore, MD 21205, USA.
E-mail address: jhua@mri.jhu.edu (J. Hua).

https://doi.org/10.1016/j.schres.2018.10.016
0920-9964/

Abbreviations

3T – 3.0 Tesla
7T – 7.0 Tesla
SCZ – Schizophrenia
BOLD – Blood-oxygenation-level dependent
fMRI – Functional MRI
BPRS – Brief psychiatric rating scale
MoCA – Montreal cognitive assessment
GRE – Gradient-echo
EPI – Echo-planar imaging
SPM – Statistical parametric mapping
GSR – Global signal regression

needed at 3T. Here, we test this hypothesis by using resting state BOLD fMRI at 7T in a group of schizophrenia patients and matched controls to measure functional connectivity between sub-regions in the thalamus defined by the Oxford thalamic connectivity atlas (Behrens et al., 2003a; Behrens et al., 2003b) and the whole brain on a voxel-by-voxel basis.

2. Methods

2.1. Participants

Fourteen patients with a diagnosis of schizophrenia (n = 12) or schizoaffective (n = 2) disorder and fourteen age and sex matched normal controls were recruited and scanned following a Johns Hopkins Medicine Institutional Review Board approved protocol. All participants gave written informed consent before scanning. None of the subjects had other neurologic history or neurological signs on exam, or a history of vascular diseases. As tobacco smoking could potentially affect baseline brain perfusion and thus the BOLD effect, current smoking status (cigarettes smoked per day) was determined for patients and controls. Current schizophrenia symptom severity was assessed with the Brief Psychiatric Rating Scale (BPRS) (Overall and Gorham, 1962). Diagnosis was based on clinical records and clinical referrals at the point of ascertainment, and was confirmed by symptom evaluation on entry into the study. All patients, but none of the controls, were receiving antipsychotic medicines. Current chlorpromazine (CPZ) equivalents (Andreasen et al., 2010) were used as a proxy for lifetime antipsychotic exposure. The Montreal Cognitive Assessment (MoCA) (Nasreddine et al., 2005) was performed on each participant on the day of scanning.

2.2. MRI

All scans were performed on a 7T Philips MRI scanner (Philips Healthcare, Best, The Netherlands). A 32-channel phased-array head coil (Nova Medical, Wilmington, MA) was used for RF reception and a head-only quadrature coil for transmit. High-resolution anatomical images were acquired with a 3D magnetization prepared 2 rapid acquisition gradient echoes (MP2RAGE) sequence (Marques et al., 2009; Van de Moortele et al., 2009) (voxel = 0.65 mm isotropic) to minimize B1 field inhomogeneity induced artifacts at 7T. A resting state fMRI scan was performed with gradient echo (GRE) echo-planar imaging (EPI) (TR/TE/FA = 2000/22 ms/60°, voxel = 2.5 mm isotropic, 54 slices, 7 min) for each participant.

2.3. Data analysis

The statistical parametric mapping (SPM) software package (Version 8, Wellcome Trust Centre for Neuroimaging, London, United Kingdom; http://www.fil.ion.ucl.ac.uk/spm/) and in-house code programmed in Matlab (MathWorks, Natick, MA, USA) were used for image analysis. Preprocessing included realignment, slice time correction, co-registration, segmentation, normalization; nuisance removal (CompCor) (Muschelli et al., 2014), regression of global mean and motion parameters (6 rigid body motion correction parameters computed from the SPM realignment routine, and the first derivative of each parameter); and temporal filtering (0.01–0.1 Hz). Given the emerging concerns that micro movements can affect between group differences in functional connectivity data even after standard motion correction procedures (Power et al., 2012; Satterthwaite et al., 2012; Van Dijk et al., 2012), we applied an additional "scrubbing" procedure described in previous works (Muschelli et al., 2014; Power et al., 2012). Briefly, the 6 rigid body motion correction parameters were converted into the Framewise Displacement (FD) (Power et al., 2012) by summing the absolute value of the 3 differenced translational parameters and the 3 differenced rotational parameters. An FD threshold of 0.5 mm was used to identify potentially motion-contaminated scans, and one scan before and 2 scans after each of these scans above the FD threshold were excluded from further analysis. All analysis was also repeated without the global signal regression (GSR) step.

To perform seed-based functional connectivity analysis between sub-thalamic regions and the brain, the Oxford thalamic connectivity atlas (Behrens et al., 2003a; Behrens et al., 2003b) was employed. This atlas was generated using diffusion based structural connectivity in white matter between the thalamus and cortex, which segments the thalamus into seven sub-regions, with >25% probability of connection to seven exclusive cortical areas, respectively (Fig. 1). Seed-based analysis was carried out using each thalamic sub-region as a seed, and whole brain connectivity maps (z values) to each seed were calculated. Second-level *t*-tests were performed to examine differential connectivity between schizophrenia patients and controls in the whole brain. Age, sex, smoking status, regional gray matter volume from anatomical scans, motion and differential motion parameters were all accounted for as covariates in the analysis. Significant clusters of decreased or increased thalamic connectivity were identified using threshold-free cluster enhancement (Smith and Nichols, 2009). The IBASPM116 atlas (Lancaster et al., 1997; Lancaster et al., 2000; Maldjian et al., 2004; Maldjian et al., 2003; Tzourio-Mazoyer et al., 2002) (PickAtlas software, Wake Forest University, North Carolina, USA) was used to identify anatomical regions within the significant clusters (note that an anatomical region from the atlas may have both decreased or increased connectivity clusters in its sub-regions). Effect size was estimated with Cohen's d. Correlations between thalamic connectivity and disease duration, antipsychotic medication dosage, BPRS and MoCA scores (including the total score and subscales for both BPRS and MoCA) were evaluated using adjusted R^2 from linear regression. Note that for correlations between thalamic connectivity and disease duration, BPRS and MoCA scores, partial correlations were calculated with age, smoking status and medication dosage as covariates. Multiple comparisons in the correlation analysis (functional connectivity between the thalamus and multiple cortical regions) were corrected for with the false-discovery rate (adjusted $P < 0.05$) (Rosner, 2011).

3. Results

Demographic information and clinical measures are shown in Table 1. Age and sex were matched between schizophrenia patients and control subjects ($P > 0.1$). The average numbers of cigarettes smoked per day were comparable between the two groups. Schizophrenia patients had significantly higher BPRS scores ($P < 0.001$), and slightly lower total MoCA scores ($P < 0.05$) compared to control subjects. No significant differences were found in motion parameters derived from the SPM realignment routine between the two groups (data not shown).

Tables 2 and 3 summarize the main findings in the group comparisons. Hyper-connectivity (Table 2) and hypo-connectivity (Table 3)

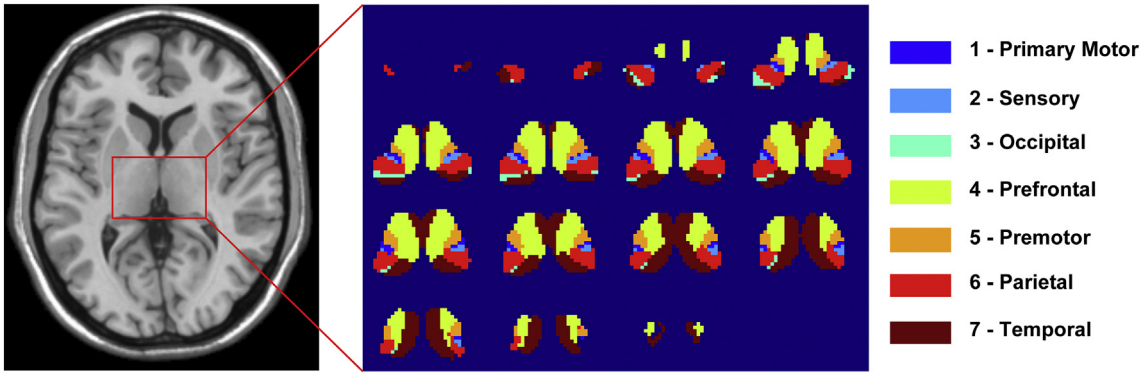

Fig. 1. Oxford thalamic connectivity atlas. The thalamus is segmented into seven sub-regions based on white matter diffusion tractography. Each sub-region has a primary connection to a cortical area as listed in the Figure.

between thalamic sub-regions and various cortical areas were detected in schizophrenia patients compared to controls, which include both primary targets and other regions (non-primary, shaded in Tables 2 and 3) of each seed. Hyper-connectivity was observed between all thalamic sub-regions and the sensory/motor cortex and the temporal cortex. Hyper-connectivity to some regions in the parietal cortex was also detected from several thalamic sub-regions. Hypo-connectivity in schizophrenia patients was found between thalamic sub-regions and the frontal cortex, the cingulate cortex, the caudate and putamen, and the cerebellum. Most of these changes were detected in both hemispheres in corresponding regions, although the cluster sizes varied between the left and right hemispheres in some regions. Fig. 2 displays the regions with significantly decreased or increased thalamic functional connectivity in schizophrenia patients compared to controls on MNI normalized anatomical images (significant regions from each sub-thalamic seed combined on the same figure).

Significant positive correlation was found between disease duration in schizophrenia patients and functional connectivity between the thalamus and the sensory/motor cortex (Fig. 3). Significant negative correlation was observed between disease duration and functional connectivity between the thalamus and the prefrontal cortex (Fig. 3). Age, smoking status and medication dosage were included as covariates in the correlation analysis. Note that here all sub-thalamic regions that showed significant difference in functional connectivity with the sensory/motor or the prefrontal cortex in the group comparisons were combined (union) in the correlation analysis, as results from individual seed region did not survive the significance tests, possibly due to insufficient sensitivity. The disease durations of the fourteen patients included in this analysis can be split into two sub-groups with moderate (n = 8) or long (n = 6) disease duration. However, the sample size of each sub-group was too small to detect significant differences between them. Functional connectivity did not significantly correlate with BPRS or MoCA scores (including subscales for both BPRS and MoCA), or antipsychotic medication dosage in schizophrenia patients.

Functional connectivity between the thalamus and the sensory/motor cortex, and functional connectivity between the thalamus and the prefrontal cortex also showed significant negative correlation (Fig. 4). Here, all sub-thalamic regions that showed significant difference in functional connectivity with the sensory/motor or the prefrontal cortex in the group comparisons were also combined as Fig. 3.

The key findings including group differences and correlations remained significant when all analysis was repeated without global signal regression (GSR). The results without GSR are reported in Supplemental Tables S2 and S3.

Table 1
Demographic and clinical data for the study participants.

	Control subjects	Schizophrenia patients	P value[a]
N	14	14	N/A
Sex (Male)	75%	75%	1
Race (Caucasian/African American)	7/7	7/7	1
Age (year)	37.3 ± 16.7[b]	39.5 ± 18.5	0.71
Disease duration (year)	N/A	19.1 ± 17.7	N/A
Smoking status (cig/day)	1.7 ± 3.1	2.3 ± 2.4	0.55
BPRS score[c]	23.1 ± 3.4	38.1 ± 8.4	<0.00001
Medication[d]	N/A	93.9 ± 130.7	N/A
MoCA[e] score	25.5 ± 3.0	22.8 ± 3.8	0.04

[a] P values from two-sample t-tests between the two groups for age, smoking status, BPRS and MoCA scores; or from $\chi 2$-test for the categorical variable sex.
[b] Mean ± standard deviation.
[c] Brief Psychiatric Rating Scale (BPRS); please see Methods section for references.
[d] Medication reported with derived chlorpromazine equivalent dose in dose-year (milligram). More detailed information about medication doses and types are reported in Supplemental Table S1. Current chlorpromazine (CPZ) equivalents (Andreasen et al., 2010) were used as a proxy for lifetime antipsychotic exposure.
[e] Montreal Cognitive Assessment (MoCA); please see Methods section for references.

4. Discussion

In this study, resting state BOLD fMRI was performed at 7T to examine functional connectivity between sub-thalamic regions and the other brain areas in schizophrenia patients. Our results showed impaired thalamic connectivity to the prefrontal cortex and the cerebellum, but enhanced thalamic connectivity to the motor/sensory cortex in schizophrenia. The negative correlation between the hyper-connectivity in the thalamus-sensory/motor circuit and the hypo-connectivity in the thalamus-prefrontal circuit may imply a compensatory mechanism in the brain, where additional cortical regions are recruited to subserve functions that have been impaired due to the pathology of the disorder (Anticevic et al., 2014; Anticevic et al., 2015). We also found significant correlations between altered functional connectivity and disease duration in the patients. Our main findings (altered thalamic connectivity to the cortex) in the current study are consistent with previous large scale studies conducted at 3T and lower fields (Anticevic et al., 2014; Anticevic et al., 2015; Cetin et al., 2014; Klingner et al., 2014). In the present study, we were able to detect comparable effect sizes with a much smaller cohort (n = 14, as compared to n = 90 in (Anticevic et al., 2014) and n = 222 in (Anticevic et al., 2015)). We attribute this primarily to the enhanced sensitivity of BOLD fMRI at higher magnetic field.

We used the Oxford thalamic connectivity atlas (Behrens et al., 2003a; Behrens et al., 2003b) to define the seed regions within the thalamus for the functional connectivity analysis in this study. Each sub-region (seed) in this atlas has a primary anatomical connection based on a probability threshold of 25% calculated from diffusion MRI measures. Therefore, many voxels within one sub-region can still have anatomical connections to brain regions other than their assigned primary target (Behrens et al., 2003a; Johansen-Berg et al., 2005). This seems to

Table 2
Hyper-connectivity (schizophrenia > control) between thalamic sub-regions and various brain regions in schizophrenia patients compared to controls.

			Functional connectivity (z)									
			Schizophrenia		Control			Cluster peak[d] (mm, MNI)				
Region[a]	Hemisphere	Cluster size[b]	Mean	std	Mean	std	Effect size[c]	x	y	z	Peak T	Adjusted P value
Sub–region 1 (connection to primary motor)												
Precentral	R	120	0.096	0.059	–0.046	0.077	2.15	–42	–8	46	5.03	1e–5
Precentral	L	97	0.043	0.036	–0.062	0.057	2.29	34	–4	50	4.47	0.001
Paracentral_Lobule	L	60	0.082	0.065	–0.047	0.066	2.04	10	–30	62	4.36	0.004
Parietal_Sup	L	50	0.016	0.063	–0.066	0.056	1.43	24	–64	48	5.44	0.001
Postcentral	R	140	0.069	0.054	–0.056	0.075	1.99	–38	–30	50	4.83	1e–5
Postcentral	L	112	0.055	0.042	–0.063	0.055	2.50	22	–46	56	5.01	0.007
Precuneus	L	55	0.043	0.035	–0.059	0.043	2.70	6	–64	54	4.53	0.002
Supp_Motor_Area	R	71	0.092	0.063	–0.041	0.055	2.33	–8	–22	62	4.02	1e–5
Supp_Motor_Area	L	87	0.100	0.066	–0.035	0.066	2.12	8	–16	56	5.07	0.003
Temporal_Mid	R	95	0.036	0.064	–0.093	0.051	2.31	–42	–66	0	4.50	0.007
Temporal_Sup	R	82	0.053	0.045	–0.043	0.075	1.61	–52	–36	8	5.08	0.001
Sub–region 2 (connection to sensory)												
Postcentral	R	150	0.072	0.054	–0.055	0.069	2.13	–52	–8	36	5.25	0.001
Postcentral	L	194	0.048	0.041	–0.070	0.067	2.20	50	–10	20	4.71	1e–5
SupraMarginal	R	23	0.054	0.063	–0.051	0.065	1.70	–38	–32	40	3.93	1e–5
SupraMarginal	L	52	0.029	0.027	–0.048	0.062	1.67	52	–26	14	4.05	0.002
Paracentral_Lobule	L	74	0.073	0.058	–0.053	0.073	1.98	10	–30	60	5.71	0.009
Precentral	R	170	0.100	0.065	–0.047	0.082	2.06	–42	4	30	4.66	0.005
Precentral	L	130	0.036	0.033	–0.062	0.065	1.97	52	4	28	4.86	0.001
Supp_Motor_Area	R	161	0.090	0.058	–0.034	0.070	2.00	–12	14	46	5.57	0.001
Supp_Motor_Area	L	122	0.088	0.058	–0.034	0.071	1.95	8	–14	48	4.18	0.001
Temporal_Mid	L	178	0.014	0.024	–0.074	0.054	2.19	58	–16	–18	4.60	1e–5
Temporal_Sup	L	144	0.047	0.045	–0.064	0.083	1.73	50	–28	12	4.99	0.001
Sub–region 3 (connection to occipital)												
Postcentral	R	153	0.073	0.050	–0.040	0.085	1.68	–52	–4	30	4.15	0.001
Precentral	R	128	0.090	0.056	–0.039	0.085	1.86	–48	–8	38	4.88	0.007
Temporal_Sup	R	92	0.042	0.041	–0.024	0.096	0.93	–54	–10	–12	4.46	0.009
Sub–region 4 (connection to prefrontal)												
Postcentral	R	81	0.060	0.046	–0.042	0.074	1.72	–26	–42	56	4.40	1e–5
Postcentral	L	55	0.037	0.041	–0.063	0.068	1.85	20	–32	58	4.04	1e–5
Precentral	R	94	0.090	0.080	–0.036	0.070	1.74	–50	4	34	5.03	1e–5
Precentral	L	40	0.025	0.036	–0.076	0.069	1.90	56	0	34	4.71	1e–5
Supp_Motor_Area	R	36	0.054	0.079	–0.033	0.053	1.34	–12	0	52	3.91	0.002
Temporal_Mid	L	37	–0.008	0.038	–0.071	0.057	1.35	52	–48	6	5.41	0.002
Temporal_Mid	R	27	0.025	0.051	–0.052	0.044	1.68	–52	–64	6	3.17	1e–5
Sub–region 5 (connection to premotor)												
Precentral	R	169	0.099	0.061	–0.050	0.082	2.14	–44	2	38	5.15	1e–5
Precentral	L	153	0.039	0.030	–0.071	0.061	2.37	26	–18	64	4.58	0.003
Supp_Motor_Area	R	123	0.098	0.068	–0.037	0.063	2.14	–10	–16	60	5.64	1e–5
Supp_Motor_Area	L	121	0.100	0.064	–0.033	0.063	2.17	10	–18	60	5.61	1e–5
Paracentral_Lobule	L	80	0.080	0.060	–0.051	0.063	2.21	6	–22	58	5.11	0.002
Postcentral	R	146	0.082	0.055	–0.062	0.082	2.14	–30	–36	68	4.10	1e–5
Postcentral	L	166	0.053	0.041	–0.066	0.061	2.38	24	–34	56	5.23	0.004
Temporal_Mid	R	128	0.031	0.052	–0.094	0.048	2.59	–52	–58	0	5.11	0.005
Sub–region 6 (connection to posterior parietal)												
Paracentral_Lobule	L	39	0.076	0.055	–0.065	0.080	2.13	10	–30	60	4.48	0.003
Parietal_Inf	R	33	0.048	0.069	–0.087	0.065	2.09	–32	–46	52	4.27	0.007
Postcentral	R	256	0.090	0.065	–0.052	0.085	1.95	–52	–8	36	6.13	1e–5
Postcentral	L	286	0.044	0.045	–0.070	0.074	1.93	46	–18	34	5.32	0.003
Precuneus	L	52	0.046	0.050	–0.062	0.036	2.57	20	–50	2	4.20	1e–5
Precentral	R	289	0.102	0.072	–0.047	0.086	1.95	–48	–6	28	7.08	1e–5
Precentral	L	101	0.040	0.033	–0.075	0.067	2.26	50	0	40	4.20	0.008
Supp_Motor_Area	R	101	0.096	0.060	–0.038	0.061	2.30	–10	–22	64	5.53	0.002
Temporal_Mid	R	85	0.027	0.044	–0.089	0.039	2.90	–52	–66	–2	4.13	0.001
Sub–region 7 (connection to temporal)												
Temporal_Mid	L	37	0.001	0.046	–0.069	0.065	1.29	58	–44	–2	3.14	0.003
Temporal_Sup	L	31	0.020	0.051	–0.038	0.078	0.91	46	–40	12	3.80	0.030
Postcentral	R	63	0.042	0.047	–0.034	0.064	1.40	–26	–42	56	4.61	0.001
Postcentral	L	37	0.038	0.044	–0.060	0.069	1.76	38	–34	54	3.70	1e–5
Precentral	R	35	0.077	0.081	–0.035	0.075	1.49	–28	–26	52	3.89	0.001
Precentral	L	30	0.017	0.028	–0.056	0.079	1.28	48	–2	28	4.08	0.005

Table 3
Hypo-connectivity (schizophrenia < control) between thalamic sub-regions and various brain regions in schizophrenia patients compared to controls.

			Functional connectivity (z)									
			Schizophrenia		Control			Cluster Peak[d] (mm, MNI)				
Region[a]	Hemis–phere	Cluster size[b]	Mean	std	Mean	std	Effect size[c]	x	y	z	Peak T	Adjusted P value
Sub–region 1 (connection to primary motor)												
Caudate	L	133	–0.023	0.077	0.108	0.057	–2.01	10	12	18	4.65	0.002
Sub–region 2 (connection to sensory)												
Frontal_Sup	R	48	–0.059	0.029	0.039	0.035	–3.16	–16	26	54	3.92	0.003
Frontal_Sup	L	28	–0.037	0.039	0.047	0.041	–2.18	12	32	54	4.00	0.003
Sub–region 3 (connection to occipital)												
Cerebelum_8	L	71	–0.020	0.038	0.032	0.057	–1.11	42	–54	–52	4.05	0.003
Cerebelum_9	L	52	–0.021	0.048	0.048	0.077	–1.12	12	–52	–50	4.18	0.002
Sub–region 4 (connection to prefrontal)												
Frontal_Mid	L	78	–0.065	0.074	0.032	0.056	–1.53	4	17	36	3.90	0.003
Frontal_Inf_Tri	L	55	–0.066	0.067	0.033	0.081	–1.38	48	46	12	2.87	0.003
Frontal_Inf_Oper	L	52	–0.024	0.076	0.044	0.076	–0.93	60	12	22	2.81	0.003
Caudate	L	92	–0.043	0.053	0.101	0.076	–2.28	4	18	–4	4.13	0.003
Cingulate_Post	R	37	–0.025	0.063	0.094	0.072	–1.83	–4	–40	22	4.28	0.003
Sub–region 5 (connection to premotor)												
Frontal_Sup	L	33	–0.043	0.050	0.048	0.042	–2.05	14	50	38	4.33	0.003
Caudate	L	120	–0.033	0.067	0.106	0.060	–2.27	18	12	20	3.88	0.002
Sub–region 6 (connection to posterior parietal)												
Frontal_Sup	R	82	–0.062	0.034	0.045	0.038	–3.08	–22	54	10	4.89	0.002
Frontal_Mid	R	64	–0.066	0.036	0.028	0.033	–2.82	–30	50	4	4.38	0.002
Caudate	L	67	–0.045	0.062	0.102	0.068	–2.34	18	10	20	5.29	0.002
Cingulate_Mid	R	37	–0.039	0.044	0.057	0.047	–2.19	–2	–32	46	3.39	0.002
Sub–region 7 (connection to temporal)												
Cingulate_Post	R	33	0.002	0.069	0.108	0.097	–1.31	–10	–40	18	4.25	0.002

[a] The brain regions were labeled according to the IBASPM 116 atlas (please see Methods for references).
[b] Number of voxels that show significant group difference in this region.
[c] Effect size was estimated with Cohen's *d*.
[d] Location of the voxel with the maximum (peak) T-score in the cluster in the MNI space.
Shaded regions indicate non-primary targets of each seed (sub-thalamic region from the atlas).
std: inter-subject standard deviation.

be the case for functional connectivity as well. In our data, each thalamic sub-region also had functional connections to multiple brain areas other than its primary target. Similar results have been reported in previous 3T studies (Anticevic et al., 2014; Anticevic et al., 2015). Alternatively, data driven approaches can be carried out to segment the thalamus based on the functional connectivity to various brain regions (Anticevic et al., 2014; Anticevic et al., 2015). As such procedures typically require much larger sample size, they will be incorporated in our subsequent studies.

The global signal regression (GSR) step in functional connectivity analysis may potentially confound group comparison results (Murphy et al., 2009), as the magnitudes of the global brain signal may vary under different physiological and pathological conditions (Yang et al., 2014). We therefore performed the same analysis with and without the GSR step in preprocessing. Similar to reports in the literature (Murphy et al., 2009), the results without GSR seemed to show somewhat less anti-correlations compared to results with GSR. However, our main findings including the group level differences in functional connectivity and correlations were consistent between the two methods.

Regional brain atrophy, which has been documented in schizophrenia (Kreczmanski et al., 2005; Loeber et al., 1999; Meda et al., 2008; Ota et al., 2014; Pearlson et al., 1997; Walther et al., 2011), may be another potential confounding effect for the functional connectivity measures. To rule out this confounding factor, we included gray matter volume derived from high resolution anatomical images as a covariate in group comparisons and correlation analyses in this study.

Tobacco use is always more prevalent in schizophrenia patients than the general population, and chronic smoking may significantly alter brain functions. Therefore, most control subjects recruited for this study were regular smokers, in order to group match the schizophrenia patients. The current smoking status of each study participant was recorded in cigarettes smoked per day, and the average numbers were comparable between controls and patients. Moreover, smoking status was included as a covariate for all statistical analyses here. Full exploration of the effects of smoking on functional connectivity will require a more detailed investigation, including more refined measures of cigarette exposure and a sample size sufficient to search for a dose-response relationship between smoking and measures of connectivity. Note that the functional connectivity data in controls in the current study may also be different from normal subjects in other studies due to tobacco use.

Finally, an important caveat is that the patients, not controls, in this study were all receiving antipsychotic medicines. Several studies have shown that antipsychotic drugs and their therapeutic effect can restore and increase functional connectivity in the ventral tegmental area

Notes to table 2:
[a] The brain regions were labeled according to the IBASPM 116 atlas (please see Methods for references).
[b] Number of voxels that show significant group difference in this region.
[c] Effect size was estimated with Cohen's *d*.
[d] Location of the voxel with the maximum (peak) T-score in the cluster in the MNI space.
Shaded regions indicate non-primary targets of each seed (sub-thalamic region from the atlas).std: inter-subject standard deviation.

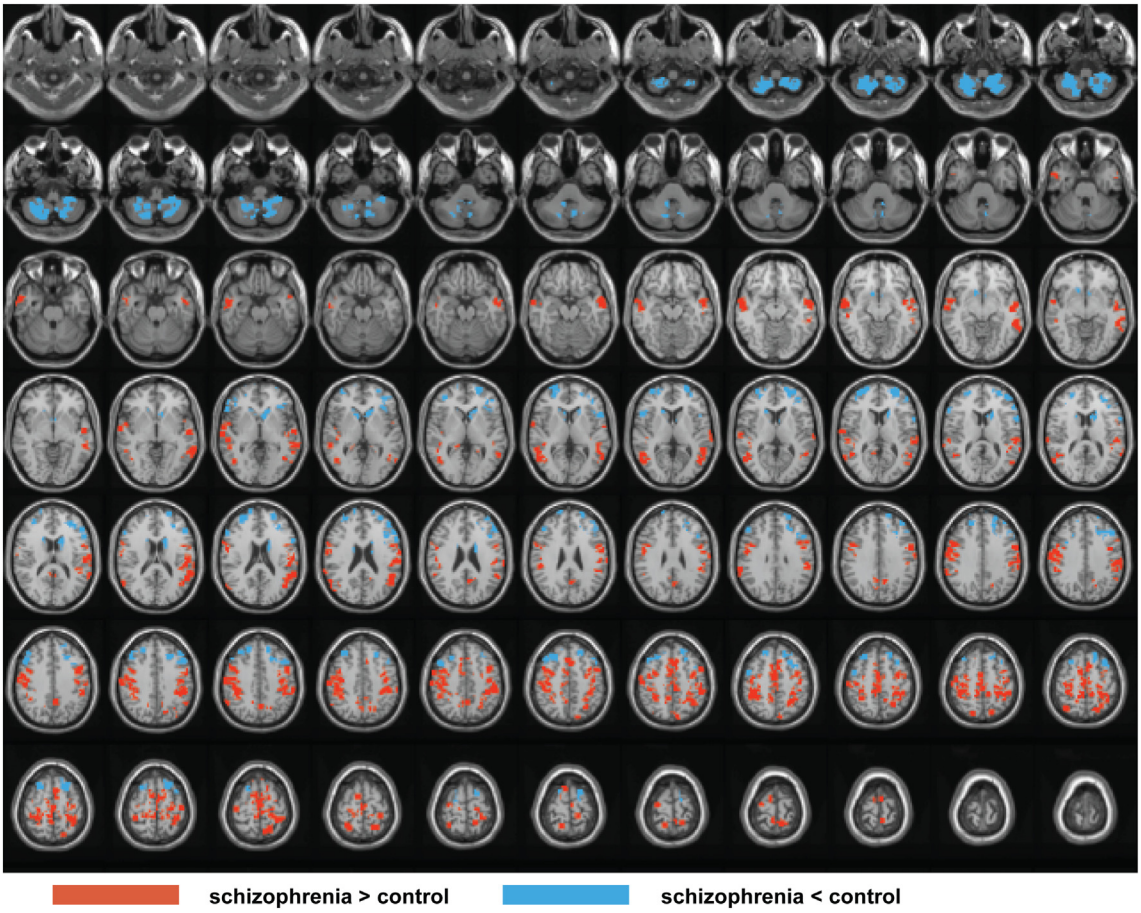

Fig. 2. Map of thalamic functional connectivity changes between schizophrenia patients and control subjects overlaid on MNI normalized anatomical images. Only voxels that show significant difference between the two groups are highlighted (red: schizophrenia > control; blue: schizophrenia < control). Significant results from all sub-thalamic seed regions in Tables 2 and 3 are shown on the same figure.

(midbrain) (Hadley et al., 2014), striatum (Sarpal et al., 2015), dorsal attention network (Kraguljac et al., 2016a), and hippocampus (Kraguljac et al., 2016b) in schizophrenia patients. A further complication is that different pharmacological classes of antipsychotics may have different effects on brain function (Goozee et al., 2014). In our data, no significant correlation was found between functional connectivity and medication dosage in patients; and medication dosage was included as a covariate when assessing correlations between functional connectivity and disease duration, BPRS and MOCA scores (including subscales). Besides, decreased functional connectivity was found between the thalamus and the prefrontal cortex, and the cerebellum, whereas the studies mentioned above showed increased functional connectivity after antipsychotic drug administration. Future study is warranted to determine if abnormalities in functional connectivity are also presenting in unmedicated patients, and if antipsychotics differentially affect connectivity of specific brain regions.

The small sample size is a fundamental limitation of the current study. The heterogeneity of the study population (the patients can be split into two sub-groups with moderate (n = 8) or long (n = 6) disease duration) and differential effects of acute and chronic substance

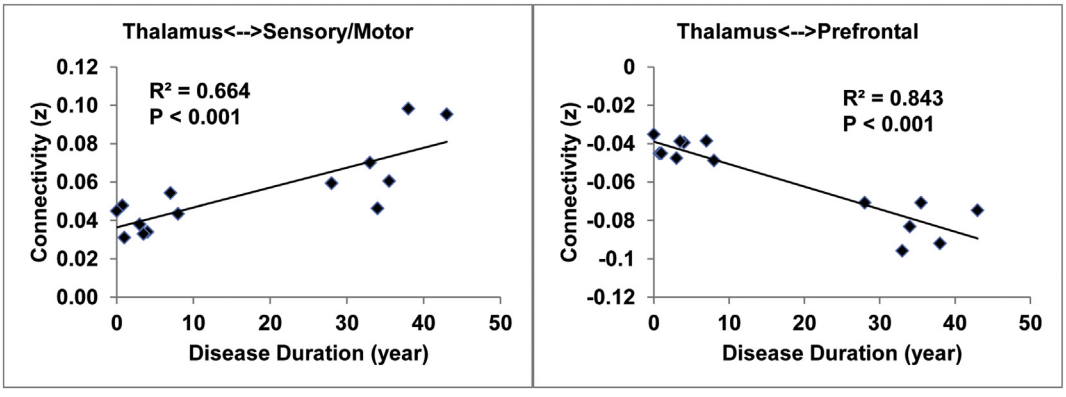

Fig. 3. Correlations analysis. Scatter plots showing correlations between the disease duration in schizophrenia patients, and the thalamic functional connectivity to the sensory/motor cortex (a) and the prefrontal cortex (b), respectively. R^2: adjusted R^2 from linear regression. Age, smoking status and medication dosage were included as covariates in the correlation analysis. All sub-thalamic regions that showed significant difference in functional connectivity with the sensory/motor or the prefrontal cortex in the group comparisons were combined in the correlation analysis.

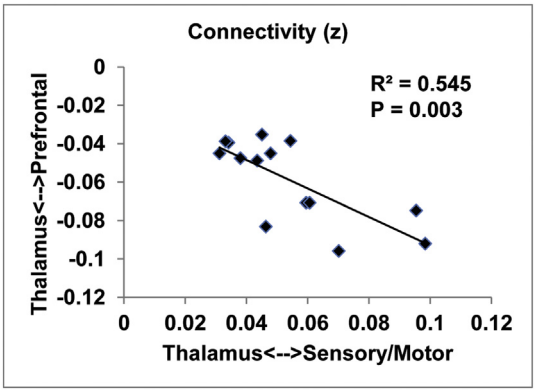

Fig. 4. Correlation between thalamic functional connectivity to the sensory/motor cortex and the prefrontal cortex. R^2: adjusted R^2 from linear regression. All sub-thalamic regions that showed significant difference in functional connectivity with the sensory/motor or the prefrontal cortex in the group comparisons were combined in the correlation analysis.

abuse other than tobacco may also confound the results of group comparisons and correlation analysis. Future studies with larger samples will be necessary to validate our findings, analyze additional clinical variables, and explore the relationship of thalamic anatomy and connectivity in further detail.

5. Conclusion

The enhanced sensitivity of BOLD fMRI at ultra-high field (7T) allowed the detection of altered functional connectivity between subregions in the thalamus and cortex in schizophrenia patients from a cohort much smaller compared to previous 3T studies. Our results therefore support the further development of ultra-high field functional connectivity measures as biomarkers for therapeutic trials in schizophrenia, which could greatly benefit from the capacity to detect functional changes with fewer subjects. In addition, our data support further investigation into the potential value of using functional connectivity, as determined by ultra-high field methods, to track disease progression and evaluate therapeutic interventions at the level of individual patients.

Supplementary data to this article can be found online at https://doi.org/10.1016/j.schres.2018.10.016.

Contributors

Jun Hua conducted data collection, data analysis and interpretation, drafting of the article, revision of the article, and final approval.

Nicholas I.S. Blair conducted the functional MRI data analysis.

Adrian Paez contributed to data analysis and revision of the article.

Ann Choe contributed to data interpretation and revision of the article.

Anita D. Barber contributed to data interpretation and revision of the article.

Allison Brandt contributed to the collection and analysis of the clinical data, and revision of the article.

Issel Anne L. *Lim* contributed to data collection.

Feng Xu contributed to data interpretation and revision of the article.

Vidyulata Kamath contributed to data interpretation and revision of the article.

James J. Pekar contributed to study design, data interpretation and revision of the article.

Peter C.M. van Zijl contributed to study design, data interpretation, and revision of the article.

Christopher A. Ross contributed to study design, data interpretation, and revision of the article.

Russell L. *Margolis* contributed to study design, data analysis and interpretation, drafting of the article, revision of the article, and final approval.

Conflict of interest

Equipment used in the study was manufactured by Philips. Peter C.M. van Zijl receives grant support from Philips, is a paid lecturer for Philips, and is the inventor of technology that is licensed to Philips. This arrangement has been approved by Johns Hopkins in accordance with its conflict of interest policies.

Role of funding source

This work was supported by NIH grants R21 MH107016 and P41 EB015909, the ABCD Charitable Trust, and a generous donation from Mr. Jose Brito.

Acknowledgments

The authors thank Mr. Joseph S. Gillen, Mrs. Terri Lee Brawner, Ms. Kathleen A. Kahl, and Ms. Ivana Kusevic for experimental assistance. This project was supported by a generous donation from Mr. Jose Brito, the ABCD Charitable Trust, and by the National Center for Research Resources and the National Institute of Biomedical Imaging and Bioengineering of the National Institutes of Health through resource grant P41 EB015909, and by the National Institute of Mental Health of the National Institutes of Health through grant R21 MH107016.

References

Andreasen, N.C., Pressler, M., Nopoulos, P., Miller, D., Ho, B.C., 2010. Antipsychotic dose equivalents and dose-years: a standardized method for comparing exposure to different drugs. Biol. Psychiatry 67 (3), 255–262.

Anticevic, A., Cole, M.W., Repovs, G., Murray, J.D., Brumbaugh, M.S., Winkler, A.M., Savic, A., Krystal, J.H., Pearlson, G.D., Glahn, D.C., 2014. Characterizing thalamo-cortical disturbances in schizophrenia and bipolar illness. Cereb. Cortex 24 (12), 3116–3130.

Anticevic, A., Haut, K., Murray, J.D., Repovs, G., Yang, G.J., Diehl, C., McEwen, S.C., Bearden, C.E., Addington, J., Goodyear, B., Cadenhead, K.S., Mirzakhanian, H., Cornblatt, B.A., Olvet, D., Mathalon, D.H., McGlashan, T.H., Perkins, D.O., Belger, A., Seidman, L.J., Tsuang, M.T., van Erp, T.G., Walker, E.F., Hamann, S., Woods, S.W., Qiu, M., Cannon, T.D., 2015. Association of thalamic dysconnectivity and conversion to psychosis in youth and young adults at elevated clinical risk. JAMA Psychiat. 72 (9), 882–891.

Behrens, T.E., Johansen-Berg, H., Woolrich, M.W., Smith, S.M., Wheeler-Kingshott, C.A., Boulby, P.A., Barker, G.J., Sillery, E.L., Sheehan, K., Ciccarelli, O., Thompson, A.J., Brady, J.M., Matthews, P.M., 2003a. Non-invasive mapping of connections between human thalamus and cortex using diffusion imaging. Nat. Neurosci. 6 (7), 750–757.

Behrens, T.E., Woolrich, M.W., Jenkinson, M., Johansen-Berg, H., Nunes, R.G., Clare, S., Matthews, P.M., Brady, J.M., Smith, S.M., 2003b. Characterization and propagation of uncertainty in diffusion-weighted MR imaging. Magn. Reson. Med. 50 (5), 1077–1088.

Cetin, M.S., Christensen, F., Abbott, C.C., Stephen, J.M., Mayer, A.R., Canive, J.M., Bustillo, J.R., Pearlson, G.D., Calhoun, V.D., 2014. Thalamus and posterior temporal lobe show greater inter-network connectivity at rest and across sensory paradigms in schizophrenia. NeuroImage 97, 117–126.

Goozee, R., Handley, R., Kempton, M.J., Dazzan, P., 2014. A systematic review and meta-analysis of the effects of antipsychotic medications on regional cerebral blood flow (rCBF) in schizophrenia: association with response to treatment. Neurosci. Biobehav. Rev. 43, 118–136.

Hadley, J.A., Nenert, R., Kraguljac, N.V., Bolding, M.S., White, D.M., Skidmore, F.M., Visscher, K.M., Lahti, A.C., 2014. Ventral tegmental area/midbrain functional connectivity and response to antipsychotic medication in schizophrenia. Neuropsychopharmacology 39 (4), 1020–1030.

Johansen-Berg, H., Behrens, T.E., Sillery, E., Ciccarelli, O., Thompson, A.J., Smith, S.M., Matthews, P.M., 2005. Functional-anatomical validation and individual variation of diffusion tractography-based segmentation of the human thalamus. Cereb. Cortex 15 (1), 31–39.

Klingner, C.M., Langbein, K., Dietzek, M., Smesny, S., Witte, O.W., Sauer, H., Nenadic, I., 2014. Thalamocortical connectivity during resting state in schizophrenia. Eur. Arch. Psychiatry Clin. Neurosci. 264 (2), 111–119.

Kraguljac, N.V., White, D.M., Hadley, J.A., Visscher, K., Knight, D., ver Hoef, L., Falola, B., Lahti, A.C., 2016a. Abnormalities in large scale functional networks in unmedicated patients with schizophrenia and effects of risperidone. NeuroImage Clin. 10, 146–158.

Kraguljac, N.V., White, D.M., Hadley, N., Hadley, J.A., Ver Hoef, L., Davis, E., Lahti, A.C., 2016b. Aberrant hippocampal connectivity in unmedicated patients with schizophrenia and effects of antipsychotic medication: a longitudinal resting state functional MRI study. Schizophr. Bull. 42 (4), 1046–1055.

Kreczmanski, P., Schmidt-Kastner, R., Heinsen, H., Steinbusch, H.W., Hof, P.R., Schmitz, C., 2005. Stereological studies of capillary length density in the frontal cortex of schizophrenics. Acta Neuropathol. 109 (5), 510–518.

Lancaster, J.L., Rainey, L.H., Summerlin, J.L., Freitas, C.S., Fox, P.T., Evans, A.C., Toga, A.W., Mazziotta, J.C., 1997. Automated labeling of the human brain: a preliminary report on the development and evaluation of a forward-transform method. Hum. Brain Mapp. 5 (4), 238–242.

Lancaster, J.L., Woldorff, M.G., Parsons, L.M., Liotti, M., Freitas, C.S., Rainey, L., Kochunov, P.V., Nickerson, D., Mikiten, S.A., Fox, P.T., 2000. Automated Talairach atlas labels for functional brain mapping. Hum. Brain Mapp. 10 (3), 120–131.

Loeber, R.T., Sherwood, A.R., Renshaw, P.F., Cohen, B.M., Yurgelun-Todd, D.A., 1999. Differences in cerebellar blood volume in schizophrenia and bipolar disorder. Schizophr. Res. 37 (1), 81–89.

Maldjian, J.A., Laurienti, P.J., Kraft, R.A., Burdette, J.H., 2003. An automated method for neuroanatomic and cytoarchitectonic atlas-based interrogation of fMRI data sets. NeuroImage 19 (3), 1233–1239.

Maldjian, J.A., Laurienti, P.J., Burdette, J.H., 2004. Precentral gyrus discrepancy in electronic versions of the Talairach atlas. NeuroImage 21 (1), 450–455.

Marques, J.P., Kober, T., Krueger, G., van der Zwaag, W., Van de Moortele, P.F., Gruetter, R., 2009. MP2RAGE, a self bias-field corrected sequence for improved segmentation and T1-mapping at high field. NeuroImage 49 (2), 1271–1281.

Meda, S.A., Giuliani, N.R., Calhoun, V.D., Jagannathan, K., Schretlen, D.J., Pulver, A., Cascella, N., Keshavan, M., Kates, W., Buchanan, R., Sharma, T., Pearlson, G.D., 2008. A large

scale (N = 400) investigation of gray matter differences in schizophrenia using optimized voxel-based morphometry. Schizophr. Res. 101 (1–3), 95–105.
Murphy, K., Birn, R.M., Handwerker, D.A., Jones, T.B., Bandettini, P.A., 2009. The impact of global signal regression on resting state correlations: are anti-correlated networks introduced? NeuroImage 44 (3), 893–905.
Muschelli, J., Nebel, M.B., Caffo, B.S., Barber, A.D., Pekar, J.J., Mostofsky, S.H., 2014. Reduction of motion-related artifacts in resting state fMRI using aCompCor. NeuroImage 96, 22–35.
Nasreddine, Z.S., Phillips, N.A., Bedirian, V., Charbonneau, S., Whitehead, V., Collin, I., Cummings, J.L., Chertkow, H., 2005. The Montreal Cognitive Assessment, MoCA: a brief screening tool for mild cognitive impairment. J. Am. Geriatr. Soc. 53 (4), 695–699.
Ota, M., Ishikawa, M., Sato, N., Okazaki, M., Maikusa, N., Hori, H., Hattori, K., Teraishi, T., Ito, K., Kunugi, H., 2014. Pseudo-continuous arterial spin labeling MRI study of schizophrenic patients. Schizophr. Res. 154 (1–3), 113–118.
Overall, J.E., Gorham, D.R., 1962. The brief psychiatric rating scale. Psychol. Rep. 10, 799–812.
Pearlson, G.D., Barta, P.E., Powers, R.E., Menon, R.R., Richards, S.S., Aylward, E.H., Federman, E.B., Chase, G.A., Petty, R.G., Tien, A.Y., 1997. Ziskind-Somerfeld Research Award 1996. Medial and superior temporal gyral volumes and cerebral asymmetry in schizophrenia versus bipolar disorder. Biol. Psychiatry 41 (1), 1–14.
Power, J.D., Barnes, K.A., Snyder, A.Z., Schlaggar, B.L., Petersen, S.E., 2012. Spurious but systematic correlations in functional connectivity MRI networks arise from subject motion. NeuroImage 59 (3), 2142–2154.
Rosner, B., 2011. Fundamentals of Biostatistics. 7th ed. Brooks/Cole, Boston, MA, USA.
Sarpal, D.K., Robinson, D.G., Lencz, T., Argyelan, M., Ikuta, T., Karlsgodt, K., Gallego, J.A., Kane, J.M., Szeszko, P.R., Malhotra, A.K., 2015. Antipsychotic treatment and functional connectivity of the striatum in first-episode schizophrenia. JAMA Psychiat. 72 (1), 5–13.
Satterthwaite, T.D., Wolf, D.H., Loughead, J., Ruparel, K., Elliott, M.A., Hakonarson, H., Gur, R.C., Gur, R.E., 2012. Impact of in-scanner head motion on multiple measures of functional connectivity: relevance for studies of neurodevelopment in youth. NeuroImage 60 (1), 623–632.
Smith, S.M., Nichols, T.E., 2009. Threshold-free cluster enhancement: addressing problems of smoothing, threshold dependence and localisation in cluster inference. NeuroImage 44 (1), 83–98.
Tzourio-Mazoyer, N., Landeau, B., Papathanassiou, D., Crivello, F., Etard, O., Delcroix, N., Mazoyer, B., Joliot, M., 2002. Automated anatomical labeling of activations in SPM using a macroscopic anatomical parcellation of the MNI MRI single-subject brain. NeuroImage 15 (1), 273–289.
Uludag, K., Muller-Bierl, B., Ugurbil, K., 2009. An integrative model for neuronal activity-induced signal changes for gradient and spin echo functional imaging. NeuroImage 48 (1), 150–165.
Van de Moortele, P.F., Auerbach, E.J., Olman, C., Yacoub, E., Ugurbil, K., Moeller, S., 2009. T1 weighted brain images at 7 Tesla unbiased for proton density, T2* contrast and RF coil receive B1 sensitivity with simultaneous vessel visualization. NeuroImage 46 (2), 432–446.
Van Dijk, K.R., Sabuncu, M.R., Buckner, R.L., 2012. The influence of head motion on intrinsic functional connectivity MRI. NeuroImage 59 (1), 431–438.
Walther, S., Federspiel, A., Horn, H., Razavi, N., Wiest, R., Dierks, T., Strik, W., Muller, T.J., 2011. Resting state cerebral blood flow and objective motor activity reveal basal ganglia dysfunction in schizophrenia. Psychiatry Res. 192 (2), 117–124.
Yang, G.J., Murray, J.D., Repovs, G., Cole, M.W., Savic, A., Glasser, M.F., Pittenger, C., Krystal, J.H., Wang, X.J., Pearlson, G.D., Glahn, D.C., Anticevic, A., 2014. Altered global brain signal in schizophrenia. Proc. Natl. Acad. Sci. U. S. A. 111 (20), 7438–7443.